

RESEARCH PAPER

Improving the estimation of mesophyll conductance to CO₂: on the role of electron transport rate correction and respiration

Samuel C.V. Martins¹, Jeroni Galmés², Arántzazu Molins² and Fábio M. DaMatta^{1,*}

¹ Departamento de Biologia Vegetal, Universidade Federal de Viçosa, 36570-000 Viçosa, MG, Brazil

² Research Group on Plant Biology under Mediterranean Conditions, Universitat de les Illes Balears, Ctra. de Valldemossa, km 7.5, 07071, Palma, Balearic Islands, Spain

*To whom correspondence should be addressed. E-mail: fdamatta@ufv.br

Received 8 February 2013; Revised 15 April 2013; Accepted 14 May 2013

Abstract

Mesophyll conductance (g_m) can markedly limit photosynthetic CO₂ assimilation and is required to estimate the parameters of the Farquhar–von Caemmerer–Berry (FvCB) model properly. The variable J (electron transport rate) is the most frequently used method for estimating g_m , and the correct determination of J is one of its requirements. Recent evidence has shown that calibrating J can lead to some errors in estimating g_m , but to what extent the parameterization of the FvCB model is affected by calibrations is not well known. In addition to determining the FvCB parameters, variants of the J calibration method were tested to address whether varying CO₂ or light levels, possible alternative electron sinks, or contrasting leaf structural properties might play a role in determining differences in $\alpha\beta$, the product of the leaf absorptance (α) and the photosystem II optical cross-section (β). It was shown that differences in $\alpha\beta$ were mainly attributed to the use of A/C_i or $A/PPFD$ curves to calibrate J . The different $\alpha\beta$ values greatly influenced g_m , leading to a high number of unrealistic values in addition to affecting the estimates of the FvCB model parameters. A new approach was devised to retrieve leaf respiration in the light from combined A/C_i and A/C_c curves and a framework to understand the high variation in observed g_m values. Overall, a background is provided to decrease the noise in g_m , facilitating data reporting and allowing better retrieval of the information presented in A/C_i and A/C_c curves.

Key words: A/C_i curve fitting, chlorophyll fluorescence, *Coffea arabica*, *Limonium gibertii*, *Nicotiana tabacum*, variable J method.

Introduction

Photosynthesis is a major process that affects plant growth and crop productivity. In addition to stomatal and biochemical factors, the photosynthetic capacity of leaves is also determined by the mesophyll conductance (g_m), which regulates the CO₂ flux from the intercellular airspaces to the sites of carboxylation in the chloroplastic stroma (Flexas *et al.*, 2012). Early gas exchange studies assumed infinite and constant g_m , implying that the CO₂ concentrations in the substomatal cavities (C_i) and chloroplasts (C_c) would be the same (Farquhar *et al.*, 1980). However, the role of finite g_m limiting photosynthesis in response to several biotic and abiotic stresses (Flexas

et al., 2008), as well as its importance in constraining maximum photosynthetic rates, particularly in evergreen sclerophylls (Warren *et al.*, 2004; Niinemets *et al.*, 2011), is now well established. Actually, there is a general consensus that g_m must be incorporated into the Farquhar–von Caemmerer–Berry (FvCB) model of leaf photosynthesis (Farquhar *et al.*, 1980) because this model underestimates the maximum Rubisco carboxylation rate (V_{cmax}) when g_m is considered to be infinite (Ethier and Livingston, 2004; Niinemets *et al.*, 2009a).

Several methods to estimate g_m have been reported (Warren, 2006; Pons *et al.*, 2009). Among them, those based

on gas exchange coupled with the chlorophyll fluorescence technique have been extensively used. In particular, the variable J method (where J stands for electron transport rate, usually measured using chlorophyll fluorescence analysis) is the most widespread method because it allows the point-specific estimation of g_m as well as tracking how g_m supposedly changes in response to varying light or CO_2 (Pons *et al.*, 2009). However, the variable J method is highly sensitive to errors in some parameters, especially the CO_2 compensation point in the absence of photorespiration (Γ^*) and J (Harley *et al.*, 1992). Importantly, J needs to be calibrated due to the uncertainties in both the leaf absorptance (α) and photosystem II (PSII) optical cross-section (β).

The J calibration is based on the analysis of response curves of photosynthetic rates to light [A /photosynthetic photon flux density (PPFD)] or CO_2 (A/C_i) under non-photorespiratory conditions, typically under low (1–2%) oxygen conditions. Under these circumstances, the relationship between J calculated through gas exchange (J_A) and chlorophyll fluorescence (J_F) is expected to be linear because electron transport flow is primarily associated with Rubisco carboxylation. Consequently, J_A can be calculated as $J_A = 4(A + R_L)$ (Warren, 2006). Other assumptions are that $\alpha\beta$ or light respiration (R_L) values do not change in response to varying C_i or PPFD. To date, three different approaches have been used to calibrate J : the relationship between the quantum yield of PSII (Φ_{PSII}) and CO_2 (Φ_{CO_2}) (Valentini *et al.*, 1995), the relationship between J_A and J_F (Pons *et al.*, 2009), and the plot of A versus PPFD $\Phi_{\text{PSII}}/4$, which is also used to estimate R_L (Yin *et al.*, 2009). Another point deserving attention is the use of A /PPFD or A/C_i curves under low O_2 to perform the calibration; ideally, both curves should give the same results. However, as observed by Yin *et al.* (2009), fundamental differences exist when choosing A /PPFD or A/C_i curves to calibrate J . First, when using the full A/C_i curve, photorespiration can still occur at low CO_2 levels. Alternatively, the excess of energy can increase the rate of alternative electron flow. Both cases can compromise the linearity of the relationship between J_A and J_F . The same problem occurs in A /PPFD curves, where higher PPFD intensities can induce alternative electron flow (depending on g_s , low C_i can occur as well). To overcome this problem, Yin *et al.* (2009) recommended using the electron transport-limited regions of both curves, namely the combination of low light levels from A /PPFD and high C_i levels from A/C_i , which would ultimately minimize the risk of photorespiration and alternative electron flow.

More recently, Gilbert *et al.* (2012) examined the use of A /PPFD or A/C_i curves to calibrate J and demonstrated dramatic changes in g_m values estimated using either the A /PPFD or A/C_i curves. However, to what extent these calibrations affect estimates of photosynthetic parameters such as V_{cmax} or J_{max} , and whether this effect is dependent on the species studied, remain unresolved. Flexas *et al.* (2007) found no differences using both calibrations for tobacco, and extrapolated this result to other species where only the A /PPFD calibration was used. Hassiotou *et al.* (2009), using the calibration based on A/C_i curves performed under two light levels, concluded that calibration is light dependent.

Other studies did not use the A /PPFD or A/C_i calibration, but estimated α using integrating spheres and assumed a β value of 0.5 (e.g. Galmés *et al.*, 2007; Tosens *et al.*, 2012), even though β has been reported to vary (Laisk and Loreto, 1996). Collectively, these results reveal no consensus on how to calibrate J , even though g_m estimated by the variable J method is mainly dependent on J . In addition, because the fluorescence signal primarily emanates from the upper mesophyll layers, but gas exchange parameters are volume based (Warren *et al.*, 2006), measured J and estimated g_m are most probably less representative of the whole leaf in species with lower specific leaf area (SLA; leaf area per unit dry mass).

The main questions asked in this study were as follows. (i) How do the J calibrations affect g_m ? (ii) How might these calibrations be translated into the FvCB parameters? (iii) Would the calibrations be dependent on species? To answer these questions, measurements were carried out using three species with contrasting SLA and photosynthetic capacities. The results highlight how g_m , V_{cmax} , and J_{max} may be affected by using A/C_i or A /PPFD curves under low O_2 to calibrate J . The results are discussed in the context of current models of g_m estimations.

Materials and methods

Plant material and growth conditions

Limonium gibertii (Senn.) Senn. and *Nicotiana tabacum* L. seeds were germinated, and plants were grown outdoors under typical Mediterranean climate conditions (Balearic Islands, Spain, 39°38'N, 2°38'E, 85 m a.s.l.) in 4 litre pots with a commercial substrate (horticultural peat) and perlite at a proportion of 4:1. Seedlings of *Coffea arabica* L. obtained from seeds were grown outdoors under subtropical conditions in Viçosa (20°45'S, 42°15'W, 650 m a.s.l.), southeastern Brazil, using 12 litre pots containing a mixture of soil, sand, and composted manure (4:1:1, v/v/v). Plants were irrigated and fertilized as required. Measurements were performed during the summer (growing season) on ~1-year-old plants in the case of *C. arabica* and *L. gibertii*, and 1-month-old plants in the case of *N. tabacum*, on 4–6 plants per species.

Gas exchange and fluorescence measurements

Leaf gas exchange and chlorophyll a fluorescence were measured simultaneously with an open-flow infrared gas-exchange analyser system equipped with a leaf chamber fluorometer (LI-6400XT, Li-Cor, Lincoln, NE, USA). Environmental conditions in the leaf chamber consisted of a leaf-to-air vapour pressure deficit of 1.2–2.0 kPa and a leaf temperature of 25 °C.

In light-adapted leaves, the actual Φ_{PSII} was determined by measuring steady-state fluorescence (F_s) and maximum fluorescence during a light-saturating pulse of ~8000 $\mu\text{mol m}^{-2} \text{s}^{-1}$ (F_m'), following the procedures of Genty *et al.* (1989):

$$\Phi_{\text{PSII}} = (F_m' - F_s) / F_m' \quad (1)$$

The electron transport rate (J_F) was then calculated as:

$$J_F = \alpha\beta \text{ PPFD } \Phi_{\text{PSII}} \quad (2)$$

where PPFD is the photosynthetically active photon flux density, α is the leaf absorptance, and β is the PSII optical cross-section. The product $\alpha\beta$ was determined from the relationship between Φ_{PSII} and Φ_{CO_2} or A and PPFD $\Phi_{\text{PSII}}/4$, obtained by varying either the light

intensity or the CO₂ concentration under non-photorespiratory conditions in an atmosphere containing <1% O₂ (Valentini *et al.*, 1995; Yin *et al.*, 2009).

Four to six A/C_i and $A/PPFD$ curves under <1% O₂ ($A/PPFD$ and A/C_i) or 21% O₂ (only A/C_i) were obtained from different plants for each species. In light-adapted leaves, A/C_i curves were initiated at an ambient CO₂ concentration (C_a) of 400 $\mu\text{mol mol}^{-1}$ under a saturating PPFD of 1500 $\mu\text{mol m}^{-2} \text{s}^{-1}$. Once steady state was reached, C_a was decreased stepwise down to 50 $\mu\text{mol mol}^{-1}$ air. Upon completion of the measurements at low C_a , it was returned to 400 $\mu\text{mol mol}^{-1}$ air to restore the original A . Next, C_a was increased stepwise to 2000 $\mu\text{mol mol}^{-1}$ air. For the $A/PPFD$ curves, C_a was held at 400 $\mu\text{mol mol}^{-1}$, and the curve was initiated at a PPFD of 1500 $\mu\text{mol m}^{-2} \text{s}^{-1}$; then, PPFD levels were decreased to 0 $\mu\text{mol m}^{-2} \text{s}^{-1}$. Both the A/C_i and $A/PPFD$ curves consisted of 11–13 different C_a values or PPFD intensities.

C_c was calculated after Harley *et al.* (1992) as:

$$C_c = \{\Gamma^*[J_F + 8(A + R_L)]\} / [J_F - 4(A + R_L)] \quad (3)$$

where Γ^* was determined from the *in vitro* Rubisco specificity factor ($S_{c/o}$) (see below) as:

$$\Gamma^* = O/S_{c/o} \quad (4)$$

A was taken from gas-exchange measurements, and the J_F values were obtained from chlorophyll a fluorescence yield. The rate of mitochondrial respiration at darkness (R_{dark}) was measured early in the morning in dark-adapted leaves, and it was divided by two ($R_{\text{dark}}/2$) to serve as a proxy for R_L .

After estimating C_c , g_m was calculated as follows (Harley *et al.*, 1992):

$$g_m = A/(C_i - C_c) \quad (5)$$

From the A/C_i and A/C_c curves, the maximum carboxylation capacity (V_{cmax}) and maximum capacity for electron transport rate (J_{max}) were calculated on a C_i and C_c basis using the kinetic parameters of Rubisco described below and, for comparative purposes, those described in Bernacchi *et al.* (2002). The FvCB model was fitted to the data by applying iterative curve fitting (minimum least square difference) using the Microsoft Excel Solver tool (Microsoft Corporation, Redmond, WA, USA). Additionally, g_m , V_{cmax} , and J_{max} were estimated using the Ethier and Livingston (2004) method, which is based on fitting A/C_i curves with a non-rectangular hyperbola version of the FvCB model, relying on the hypothesis that g_m reduces the curvature of the Rubisco-limited portion of an A/C_i response curve. For the method based on fitting A/C_i curves, species-specific $S_{c/o}$ values were used as in the Harley method. Corrections for the leakage of CO₂ and water vapour into and out of the leaf chamber of the Li-6400–40 have been applied to all gas-exchange data, as described by Rodeghiero *et al.* (2007). The percentage corrections applied to CO₂ and water vapour flux rates are shown in Supplementary Table S1 available at JXB online for the different species.

Calibration relationships

The relationship between J_A and J_F was calibrated using the linear plot of Φ_{PSII} and Φ_{CO_2} , based on Valentini *et al.* (1995):

$$\Phi_{\text{PSII}} = k \Phi_{\text{CO}_2} + b \quad (6)$$

$$J_F = 4(\Phi_{\text{PSII}} - b) \text{ PPFD}/k \quad (7)$$

where $4/k = \alpha\beta$. k and b were obtained through the linear fit of Φ_{PSII} versus Φ_{CO_2} .

In addition, the method based on Yin's approach was also used (Yin *et al.*, 2009), which presents a straightforward way to derive $\alpha\beta$ and R_L , as follows:

$$J_A = 4(A + R_L) \quad (8)$$

$$J_F = \alpha\beta \text{ PPFD } \Phi_{\text{PSII}} \quad (9)$$

J_A is rewritten as

$$A = J_A/4 - R_L \quad (10)$$

Assuming $J_A = J_F$ under non-photorespiratory conditions gives

$$A = \alpha\beta \text{ PPFD } \Phi_{\text{PSII}}/4 - R_L \quad (11)$$

As Equation 11 has the form of $y = ax + b$, through the linear fit of A versus $\text{PPFD } \Phi_{\text{PSII}}/4$, R_L can be retrieved as the y -intercept, and $\alpha\beta$ can be retrieved as the slope of the regression. Notably, this equation presented by Yin *et al.* (2009) has an extension of the FvCB model to account for alternative electron fluxes in the form of pseudocyclic (f_{pseudo}) and cyclic (f_{cyc}) electron flow (see further details in Yin *et al.*, 2004):

$$A = \alpha\beta \text{ PPFD } \Phi_{\text{PSII}} \{1 - [f_{\text{pseudo}}/(1 - f_{\text{cyc}})]\} / 4 - R_L \quad (12)$$

According to the updated model, to accomplish Equation 8, not only are non-photorespiratory conditions required but also the down-regulation of alternative electron fluxes so that low values of f_{pseudo} and f_{cyc} allow Equation 12 to be as close as possible to Equation 11, thus reliably estimating $\alpha\beta$.

Four types of calibration were devised based on the approaches of Valentini and Yin described above. The first and second calibration methods were based on the $\Phi_{\text{PSII}}/\Phi_{\text{CO}_2}$ relationship, and the third and fourth methods were based on Yin *et al.* (2009) as follows:

- (i) $\Phi_{\text{PSII}}/\Phi_{\text{CO}_2}$ (A/C_i): this calibration is performed using the entire A/C_i curve under low O₂, and the PPFD level is that used in the normal A/C_i curve (i.e. 1500 $\mu\text{mol m}^{-2} \text{s}^{-1}$). The R_L value must be assumed. In this variant, the initial part of the A/C_i curve is the most susceptible region for the occurrence of alternative electron sinks due to a high reductant (ATP and NADPH) supply associated with high PPFD and a limitation on reductant use (low CO₂ and O₂). Conversely, this variant most resembles the conditions used in the normal A/C_i curve.
- (ii) $\Phi_{\text{PSII}}/\Phi_{\text{CO}_2}$ (PPFD >400 $\mu\text{mol m}^{-2} \text{s}^{-1}$): this is the variant more often reported in the literature and consists of using $A/PPFD$ curves under low O₂ and ambient CO₂. A disadvantage of this variant is that a loss of linearity occurs at low PPFD, as Φ_{CO_2} is affected disproportionately by errors in respiration estimations or by the increase in mitochondrial respiration at low light (the Kok-effect; Brooks and Farquhar, 1985). Thus, it is recommended to exclude Φ_{CO_2} values >0.05 to keep the relationship as linear as possible (Seaton and Walker, 1990; Edwards and Baker, 1993). To meet this criterion, PPFD levels below 400 $\mu\text{mol m}^{-2} \text{s}^{-1}$ had to be excluded, making this method prone to a high reductant supply (high PPFD) and intermediate reductant use (moderate CO₂ and low O₂).
- (iii) Yin (PPFD <400 $\mu\text{mol m}^{-2} \text{s}^{-1}$): this variant was originally described by Yin *et al.* (2009), and it can also be used to estimate R_L . As this method is not based on quantum efficiency plots, there is not the disadvantage of having to exclude the points at low PPFD or assume a given R_L value. Actually, it is recommended to use only the points at the linear phase of the $A/PPFD$ (corresponding to PPFD levels <400 $\mu\text{mol m}^{-2} \text{s}^{-1}$ for the species grown outdoors), which is in the range of a

lower reductant supply and where only the basal components of alternative electron sinks exist.

- (iv) Yin (PPFD <400 $\mu\text{mol m}^{-2} \text{s}^{-1}/C_i$ >500 $\mu\text{mol mol}^{-1}$ air): this method has the same advantages and assumptions of method (iii). A particularity of this approach resides in the incorporation of data from the A/C_i curve with C_i above 500 $\mu\text{mol mol}^{-1}$ air.

Retrieving the respiration value from combined A/C_i and A/C_c curves

The FvCB model predicts that A/C_i curves and their A/C_c counterparts share the same CO_2 compensation point (Γ), as this parameter is independent of g_m :

$$\Gamma = [\Gamma^* + K_c(1 + O/K_o)R_L/V_{cmax}]/(1 - R_L/V_{cmax})$$

Evans and von Caemmerer (1996) proposed that an averaged g_m can be estimated as the slope of the plot of A versus $C_i - C_c$. Because the plot goes through the origin, both A and $C_i - C_c$ must be zero, which is what occurs when Γ is shared by both A/C_i and A/C_c curves, as predicted by the FvCB model.

It was realized that for some data sets, when R_L was set in advance as required to obtain C_c , the plot of A versus $C_i - C_c$ in the region which was Rubisco limited showed good linearity, although with an intercept differing from zero. Given the predictions of the FvCB model, this difference should be attributed to a biased R_L used to calculate C_c , which in turn leads to different Γ values, as obtained from the A/C_i and A/C_c curves. Given this fact and that the Γ^* values in this study were reliably estimated from Rubisco kinetics in purified preparations, it is proposed here that R_L can be obtained as the value that makes the intercept of the plot of A versus $C_i - C_c$ equal zero. The approach was tested using ideal data sets where the respiration values used as inputs were successfully retrieved from the combined A/C_i and A/C_c curves. Consequently, for each curve, R_L was estimated as described below. First, R_L was set to be equal to $R_{\text{dark}/2}$, as set in previous studies (Niinemets *et al.*, 2005, 2006, 2009b). To maintain the plot A versus $C_i - C_c$ as linear as possible, only points in the C_i range strictly limited by Rubisco ($C_i < 200 \mu\text{mol mol}^{-1}$ air) were considered. Secondly, the new R_L was obtained as the value that forces the intercept of the plot A versus $C_i - C_c$ to be zero using the Goal Seek function available in Microsoft Excel (see Fig. 1 for an example). The new respiration value obtained in this way is hereafter referred to as $R_{A/C_i/A/C_c}$. An Excel spreadsheet (with modelled and real data) is available (see Supplementary Spreadsheet S1 at JXB online) that shows how this method was performed.

Rubisco kinetic parameters

The Rubisco kinetic parameters used in this study were measured *in vitro*, except the $S_{c/o}$ values for *N. tabacum* and *L. gibertii*, which were taken from Galmés *et al.* (2006) and Galmés *et al.* (2005), respectively. All measurements for the determination of Rubisco kinetic parameters were conducted at 25 °C. The Rubisco specificity factor was measured in highly purified extracts and using wheat Rubisco as a reference normalized to 100, following the procedures described in Galmés *et al.* (2005). The Michaelis–Menten constants for CO_2 (K_c) and O_2 (K_o) and the maximum rate for the carboxylase reaction (V_{cmax}) were measured in rapidly isolated leaf protein extracts (Sharwood *et al.*, 2008). Briefly, ~0.5 g fresh weight of leaves were ground in a mortar with 2 ml of ice-cold extraction buffer containing 100 mM Bicine (pH 8.2), 6% (w/v) polyethylene glycol (PEG) 4000, 2 mM MgCl_2 , 0.1 mM EDTA, 1 mM benzamidine, 1 mM ϵ -aminocaproic acid, 50 mM 2-mercaptoethanol, 10 mM dithiothreitol (DTT), 2 μM pepstain A, 10 μM E64, 10 μM chymostatin, 2 mM phenylmethylsulphonyl fluoride (PMSF), and 2.5% (w/v) polyvinylpyrrolidone (PVPP). The liquidized sample was clarified by centrifugation at 12 842 g for 4 min. A 1 ml aliquot of clarified extract was eluted using a Sephadex PD-10 column

(GE Healthcare, UK) pre-equilibrated with desalt buffer containing 100 mM Bicine (pH 8.2), 20 mM MgCl_2 , 10 mM DTT, 1 mM KH_2P_i , 0.5 mM EDTA, 1 mM benzamidine, 1 mM ϵ -aminocaproic acid, and 10 mM NaHCO_3 . The protein peak (in 1 ml) was supplemented with protease inhibitors (4 μM pepstain A, 20 μM E64, and 20 μM chymostatin). Of this extract, 250 μl was supplemented with 2.542 μCi $\text{NaH}^{14}\text{CO}_3$ and activated for 15 min before carboxylase measurements. The remainder was used to assay Rubisco catalytic sites. Measurements of K_c and V_{cmax} for the carboxylase activity in nitrogen or air were determined in two sets of eight vials from the amount of ^{14}C incorporated into PGA, as described elsewhere (Bird *et al.*, 1982). Each set of vials used eight different concentrations of bicarbonate chosen to provide CO_2 (aq) between 0.7 μM and 75 μM , each with a specific radioactivity of 3.7×10^{10} Bq mol^{-1} and containing 375 nmol RuBP. K_o was calculated from the relationship K_c (air) = K_c (N_2) $\times \{1 + [\text{O}_2]/K_o\}$. The concentration of Rubisco catalytic sites in the extract was measured from the stoichiometric binding of the inhibitor [^{14}C]CABP to CO_2 - Mg^{2+} -activated Rubisco active sites (Butz and Sharkey, 1989). Thereafter, the carboxylase catalytic turnover rate K_{cat}^c was obtained as $K_{cat}^c = V_{cmax}/[\text{catalytic sites}]$. The Rubisco kinetic constants are summarized in Table 1.

Statistical analyses

Data are expressed as the means \pm standard error. Student's *t*-tests were used to compare the photosynthetic parameters calculated with the different sets of Rubisco kinetic constants and to examine whether the intercepts of the regression were significantly different from zero. Linear regression and statistical analyses were carried out using Microsoft Excel.

Results

The effect of the different calibration methods on $\alpha\beta$

The four calibration methods tested here comprised scenarios ranging from a low (Yin PPFD <400 $\mu\text{mol m}^{-2} \text{s}^{-1}$) to a high reductant supply ($\Phi_{\text{PSII}}/\Phi_{\text{CO}_2}$ PPFD >400 $\mu\text{mol m}^{-2} \text{s}^{-1}$), all performed under non-photorespiratory conditions, although potentially affected by the occurrence of an alternative electron flow. Additionally, three species covering a large range in SLA (33 ± 1.4 , 14 ± 2.7 , and 9.0 ± 1.3 $\text{m}^2 \text{kg}^{-1}$ for *N. tabacum*, *C. arabica*, and *L. gibertii*, respectively) were selected to assess the extent to which structural changes might play a role in determining the $\alpha\beta$ product.

High regression coefficients were obtained for all of the relationships based on the four calibration methods ($r^2 = 0.91$ – 0.98) (Fig. 2). In contrast to expectations, no major differences in the estimation of $\alpha\beta$ were found between the methods Yin (PPFD <400 $\mu\text{mol m}^{-2} \text{s}^{-1}$) and $\Phi_{\text{PSII}}/\Phi_{\text{CO}_2}$ (PPFD >400 $\mu\text{mol m}^{-2} \text{s}^{-1}$) (Fig. 2B, C) and between $\Phi_{\text{PSII}}/\Phi_{\text{CO}_2}$ (A/C_i) and Yin (PPFD <400/ C_i >500 $\mu\text{mol mol}^{-1}$ air) (Fig. 2A, D). Thus, the inclusion of data at high PPFD or low C_i conditions that favour the prevalence of alternative electron fluxes, had slight effects on the estimated $\alpha\beta$. Instead, the major differences among the calibration methods were dependent on the type of data used to perform the calibration [i.e. A/PPFD or A/C_i curves (Table 2)]. Regardless of the studied species, the calibrations using only A/PPFD data gave lower $\alpha\beta$ values, ranging from 0.37 to 0.50, whereas those using A/C_i data produced higher $\alpha\beta$ values, ranging from 0.46 to 0.62 (Table 2). Notably, the species displaying the most contrasting SLA values (*N. tabacum* and *L. gibertii*) showed

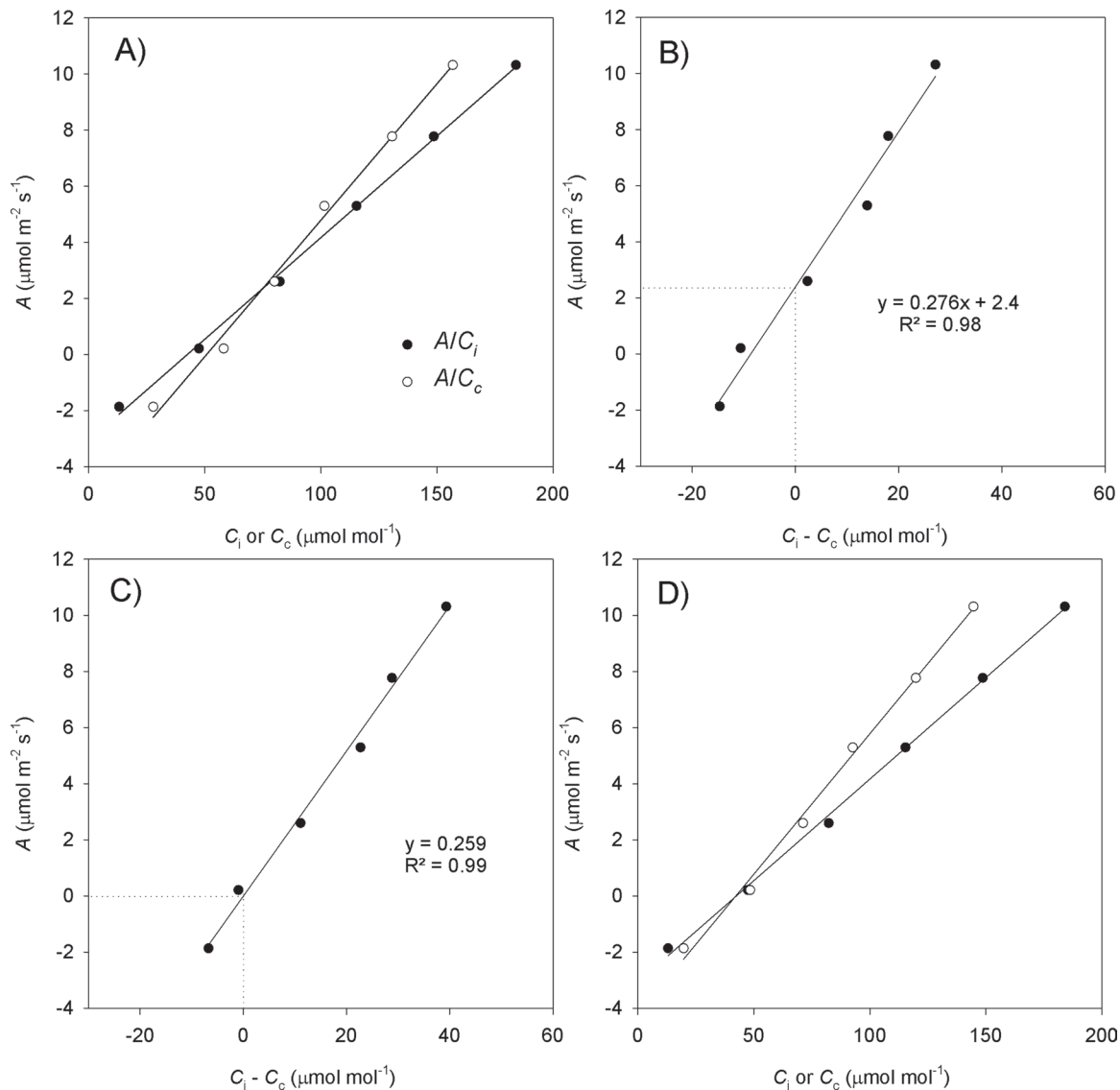


Fig. 1. Graphical representation of the method utilized to retrieve the respiration value from the combined A/C_i and A/C_c curves (R_{AC_i/AC_c}). The example is based on values measured in an *N. tabacum* leaf. (A) The initial part of an A/C_i (filled circles) and the respective A/C_c (open circles) curve considering $R_L = R_{\text{dark}/2}$ ($1.1 \mu\text{mol CO}_2 \text{ m}^{-2} \text{ s}^{-1}$). (B) $C_i - C_c$ from the curves presented in (A) plotted against A . The y -axis positive intercept (2.4) when $x=0$ (see the dotted lines) means negative g_m for A lower than the intercept because $C_i > C_c$. The slope of the linear regression (0.276) is an estimation of averaged g_m over the range of C_i used in the linear fit. (C) By adjusting to zero the intercept in the relationship A versus $C_i - C_c$, a new respiration value, R_{AC_i/AC_c} , is obtained ($0.4 \mu\text{mol CO}_2 \text{ m}^{-2} \text{ s}^{-1}$), and the same CO_2 compensation point is now shared by both curves ($C_i - C_c = 0$ at $A=0$). The influence of the new respiration on g_m can be observed as the modified slope (0.259). (D) The modified initial part of the A/C_i and A/C_c curves calculated with R_{AC_i/AC_c} .

similar values for $\alpha\beta$, suggesting that leaf structure does not play a major role in determining $\alpha\beta$.

Mesophyll conductance as affected by the J calibration methods and respiration estimations

Given that no major differences were found between the $\Phi_{\text{PSII}}/\Phi_{\text{CO}_2}$ relationship and the Yin method, g_m was estimated using the methods covering the extremes of $\alpha\beta$ values, namely $\Phi_{\text{PSII}}/\Phi_{\text{CO}_2}$ (A/C_i) and $\Phi_{\text{PSII}}/\Phi_{\text{CO}_2}$ (PPFD $>400 \mu\text{mol m}^{-2} \text{ s}^{-1}$). Because these methods consider only A/PPFD ($\Phi_{\text{PSII}}/\Phi_{\text{CO}_2}$, PPFD $>400 \mu\text{mol m}^{-2} \text{ s}^{-1}$) or A/C_i data [$\Phi_{\text{PSII}}/$

Φ_{CO_2} (A/C_i)], the g_m estimated using either method is hereafter referred to as the g_m obtained with the A/PPFD or A/C_i J calibration. Once the two J calibrations to be used were defined, an R_L value next had to be chosen to calculate C_c . Because there was no consistency in the R_L estimated via the Yin approach using A/PPFD (PPFD $<400 \mu\text{mol m}^{-2} \text{ s}^{-1}$) or A/C_i (PPFD $<400 \mu\text{mol m}^{-2} \text{ s}^{-1}$ or $C_i >500 \mu\text{mol mol}^{-1}$ air) (Table 2), $R_{\text{dark}/2}$ was preferred because it is the unique respiration value actually measured *in planta*. To check the consistency of the respiration value used, a new approach was also tested to find an alternative proxy for R_L (R_{AC_i/AC_c}) as the value forcing the CO_2 compensation point (Γ) to be equal

Table 1. Rubisco kinetic constants measured for the species studied: specificity factor ($S_{c/o}$), CO_2 compensation point in the absence of respiration (Γ^*), Michaelis–Menten kinetics for CO_2 (K_c) and O_2 (K_o), and catalytic turnover rate for the carboxylase reaction (K_{cat})

Species	$S_{c/o}$	Γ^* (μbar)	K_c (μM)	K_o (μM)	K_{cat} (s^{-1})
<i>N. tabacum</i>	98.1 ± 2.6^a	39.7 ± 1.1	12.4 ± 0.7	274 ± 42	3.2 ± 0.3
<i>C. arabica</i>	98.4 ± 4.3	39.6 ± 1.7	10.3 ± 1.3	479 ± 113	3.2 ± 0.1
<i>L. gibertii</i>	110.5 ± 1.6^b	35.2 ± 0.5	8.9 ± 0.5	593 ± 75	2.7 ± 0.8

Values are the means \pm standard error of 3–4 replicates per species.

^a Taken from Galmés et al. (2006)

^b Taken from Galmés et al. (2005).

when calculated from A/C_i and A/C_c curves. The estimated R_{AC_i/AC_c} values were always lower than their corresponding $R_{\text{dark}/2}$ counterparts (Table 3).

Due to the high amount of negative and extremely high g_m values at low or high C_i , respectively (Table 4), a filter was next applied to keep the valid g_m estimates, here defined as those values in the range of $0 < g_m < 1 \text{ mol CO}_2 \text{ m}^{-2} \text{ s}^{-1}$. As expected, the use of R_{AC_i/AC_c} significantly reduced the amount of negative values of g_m at low C_i (R_{AC_i/AC_c} in Table 4), as the rationale for this method works at this C_i range (Fig. 1). Conversely, the use of $A/C_i J$ calibration improved the g_m estimation at high C_i (Table 4) due to a lowering of C_c values (Fig. 3A). Thus, the

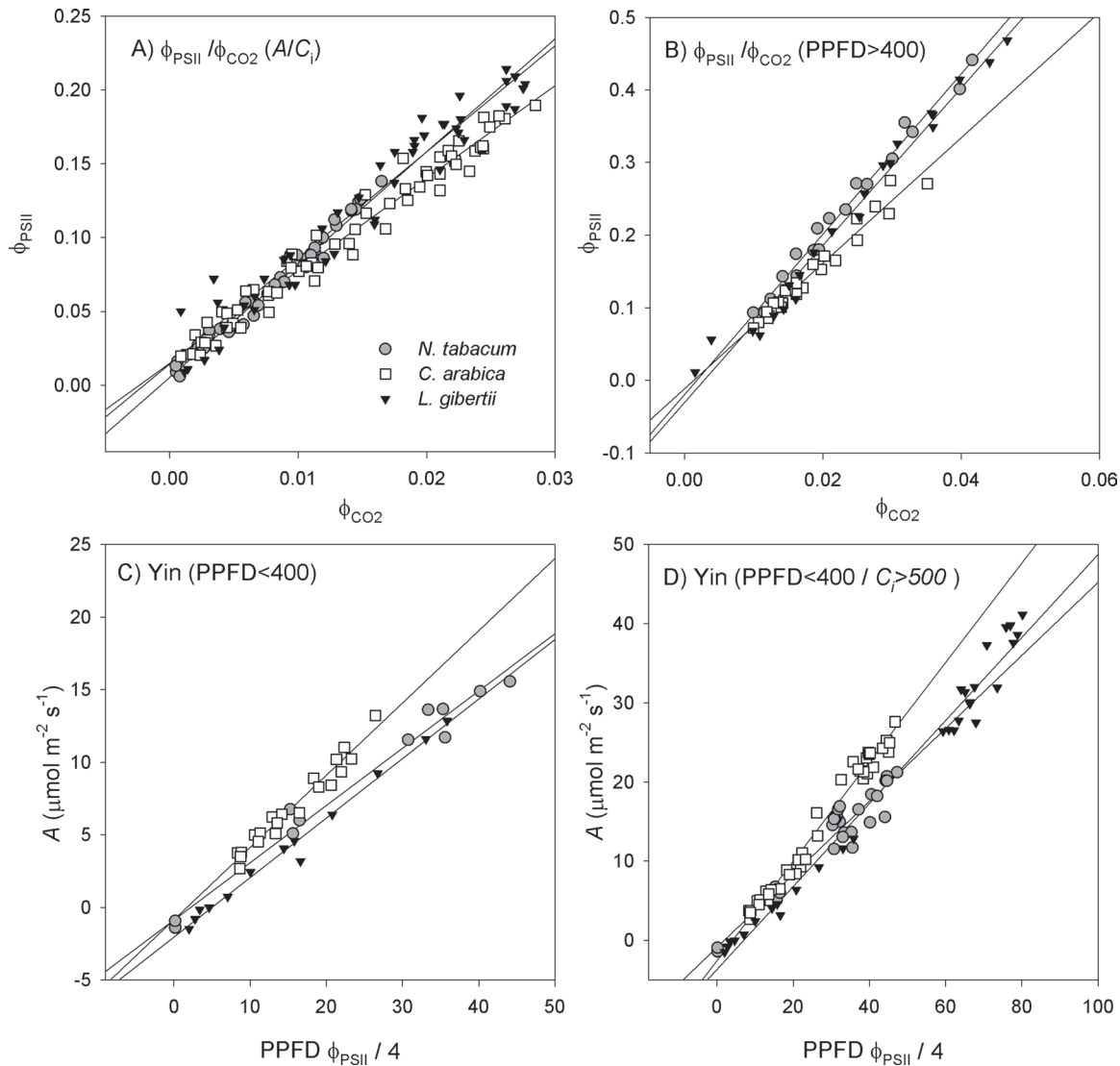


Fig. 2. Calibration relationships Φ_{PSII} versus Φ_{CO_2} (A and B) and A versus $\text{PPFD } \Phi_{\text{PSII}}/4$ (C and D) measured under non-photorespiratory conditions ($< 1\% O_2$) by varying PPFD intensities (A/PPFD curves) or substomatal CO_2 concentrations (A/C_i curves). For more details on the four calibration methods, see the Materials and methods. In (A), the entire A/C_i curve is utilized; in (B), only values at $\text{PPFD} > 400 \mu\text{mol m}^{-2} \text{ s}^{-1}$ are considered; in (C), only values at $\text{PPFD} < 400 \mu\text{mol m}^{-2} \text{ s}^{-1}$ are used; in (D), only values at $\text{PPFD} < 400 \mu\text{mol m}^{-2} \text{ s}^{-1}$ plus $C_i > 500 \mu\text{mol mol}^{-1}$ are considered. The slope of the lines in all graphs refers to the product $\alpha\beta$, whereas the y-intercept should be interpreted as the presence of alternative electron sinks in A and B and as a measure of R_L in C and D. The values of the slopes and intercepts are summarized in Table 2. Only Φ_{CO_2} values < 0.05 were kept in the plots, as recommended by Seaton and Walker (1990). The scales have different amplitudes according to the calibration. In the plots, data from 4–6 A/PPFD or A/C_i curves are used for the linear regression.

Table 2. Slopes ($\alpha\beta$) and light respiration following the method of Yin *et al.* (2011) ($R_{L,Yin}$, $\mu\text{mol CO}_2 \text{ m}^{-2} \text{ s}^{-1}$) or intercept values (Φ_{PSII}/Φ_{CO_2}) obtained under non-photorespiratory conditions according to different approaches, consisting of higher (Φ_{PSII}/Φ_{CO_2} A/C_i or PPFD >400 $\mu\text{mol m}^{-2} \text{ s}^{-1}$) or lower (Yin PPFD <400 or PPFD <400 $\mu\text{mol m}^{-2} \text{ s}^{-1}$ and C_i >500 $\mu\text{mol mol}^{-1}$ air) susceptibilities to alternative electron sinks

For comparison, the original slopes (k) obtained when using the Φ_{PSII}/Φ_{CO_2} relationship were already converted to $\alpha\beta$ ($\alpha\beta=4/k$); the intercept refers to the parameter b in the equation: $\Phi_{PSII} = k \Phi_{CO_2} + b$.

		Slope ($\alpha\beta$)	Intercept (Φ_{PSII}/Φ_{CO_2})	$R_{L,Yin}$
<i>N. tabacum</i>	Φ_{PSII}/Φ_{CO_2} (A/C _i)	0.52 ± 0.013	0.005 ± 0.002	
	Φ_{PSII}/Φ_{CO_2} (PPFD >400)	0.36 ± 0.011	-0.02 ± 0.008*	
	Yin (PPFD <400)	0.39 ± 0.017		0.87 ± 0.47
	Yin (PPFD <400 C _i >500)	0.46 ± 0.026		0.87 ± 0.87
<i>C. arabica</i>	Φ_{PSII}/Φ_{CO_2} (A/C _i)	0.64 ± 0.014	0.015 ± 0.002*	
	Φ_{PSII}/Φ_{CO_2} (PPFD >400)	0.46 ± 0.018	-0.011 ± 0.007	
	Yin (PPFD <400)	0.50 ± 0.025		0.84 ± 0.41
	Yin (PPFD <400 C _i >500)	0.63 ± 0.015		2.55 ± 0.45*
<i>L. gibertii</i>	Φ_{PSII}/Φ_{CO_2} (A/C _i)	0.56 ± 0.019	0.014 ± 0.004*	
	Φ_{PSII}/Φ_{CO_2} (PPFD >400)	0.37 ± 0.011	-0.03 ± 0.009*	
	Yin (PPFD <400)	0.41 ± 0.013		2.04 ± 0.25*
	Yin (PPFD <400 C _i >500)	0.50 ± 0.018		3.14 ± 1.02*

Values are the means ± standard error of four replicates per species.

An asterisk denotes respiration or intercepts significantly different from zero ($P < 0.05$).

Table 3. Dark respiration measured at pre-dawn (R_{dark}) and light respiration estimated from combined A/C_i and A/C_c curves (R_{AC_i/AC_c})

All values are in $\mu\text{mol CO}_2 \text{ m}^{-2} \text{ s}^{-1}$.

Species	R_{dark}	R_{AC_i/AC_c} ^a
<i>N. tabacum</i>	2.2 ± 0.1	0.3 ± 0.1
<i>C. arabica</i>	0.9 ± 0.1	0.2 ± 0.1
<i>L. gibertii</i>	4.0 ± 0.3	1.7 ± 0.4

Values are the means ± standard error of four replicates per species.

^a For R_{AC_i/AC_c} , the values are averages from the A/C_c curves calibrated using the A/PPFD or A/C_i curves.

highest percentage of data excluded (i.e. unrealistic g_m values) was found when combining the A/PPFD J calibration with $R_{dark/2}$ (88, 56, and 42% for *N. tabacum*, *C. arabica*, and *L. gibertii*, respectively), whereas the lowest percentage of data excluded was obtained with the A/C_i J calibration and R_{AC_i/AC_c} (17% for *N. tabacum* and 0% for the other species) (Table 4).

The different calibrations also affected the magnitude of g_m in response to C_i. There was no general trend at C_i <100 $\mu\text{mol mol}^{-1}$ air, whereas at C_i >100 $\mu\text{mol mol}^{-1}$ air, lower g_m values (up to 50%) were observed using the A/C_i J calibration (Table 4). In addition, when plotting g_m versus C_i, a high amplitude in g_m , depending on the calibration used, was revealed (Fig. 3B). Such amplitude led to a reasonable disagreement between the averaged g_m at C_i of 100–350 $\mu\text{mol mol}^{-1}$ air and the single point g_m at CO₂ ambient (400 $\mu\text{mol mol}^{-1}$) (Supplementary Tables S2, S3 at JXB online), which suggests that care must be exercised when reporting single point g_m data. In Supplementary Table S4, in addition to the

filter keeping the values in the range of $0 < g_m < 1 \text{ mol CO}_2 \text{ m}^{-2} \text{ s}^{-1}$, the Harley *et al.* (1992) criteria were also applied, considering the g_m data in the range of $10 < dC_i/dA < 50$ as reliable to see whether they corresponded to the data presented in Table 4. Overall, the g_m values presented in Table 4 and those obtained after applying the Harley criteria varied accordingly, but some exceptions were noticed such as the g_m values estimated at C_i >350 $\mu\text{mol mol}^{-1}$ air for *L. gibertii* which were substantially higher than the g_m data shown in Supplementary Table S4. Most importantly and irrespective of this difference, the amount of data excluded using the Harley criteria was always higher (up to 100%) even when the same estimates presented in Table 4 had 0% of data excluded together with small standard errors. Additionally, the Harley criteria worked differently depending on the species, J calibration, and C_i range, given that some species were more affected than others.

To obtain an independent estimate of g_m that was not affected by the need for calibrating J , g_m was also estimated using an alternative approach, namely the A–C_i curve analysis method suggested by Ethier and Livingston (2004). The g_m values obtained following this approach are given in Table 5.

Maximum Rubisco carboxylation and electron transport rate as affected by $\alpha\beta$

In contrast to the g_m estimates that could be greatly affected by the use of either $R_{dark/2}$ or R_{AC_i/AC_c} (Table 4, Fig. 3B), the V_{cmax} and J_{max} estimates were minimally affected by the use of different respiration values (~6% at most; Table 5; Supplementary Table S5 at JXB online).

Irrespective of species, V_{cmax} and J_{max} on a C_c basis were always higher for the A/C_i J calibration than for its A/PPFD J

Table 4. Mesophyll conductance (g_m , mol CO₂ m⁻² s⁻¹) for several intervals of C_i and percentage of data excluded (DE) after applying a restriction (g_m restricted to the range of $0 < g_m < 1$ mol CO₂ m⁻² s⁻¹)

The A/C_i or A/PPFD J calibration refers to the Φ_{PSII}/Φ_{CO_2} (A/C_i) or A/PPFD methods, respectively. R_{AC_i/AC_c} is the light respiration estimate from the combined A/C_i and A/C_c curves proposed in this study, and $R_{dark/2}$ is the dark respiration divided per two to account for the observed reduction in R_{dark} under light (Niinemets *et al.*, 2005). Note the high DE at low C_i for $R_{dark/2}$ and at high C_i for the A/PPFD J calibration.

	A/ C_i J calibration				A/PPFD J calibration			
	R_{AC_i/AC_c}		$R_{dark/2}$		R_{AC_i/AC_c}		$R_{dark/2}$	
	g_m	DE (%)	g_m	DE (%)	g_m	DE (%)	g_m	DE (%)
<i>N. tabacum</i>								
$C_i < 100$	0.290 ± 0.065	17	0.243 ± 0.033	58	0.345 ± 0.132	17	0.203 ± 0.031	67
$C_i 100-350$	0.213 ± 0.021	0	0.287 ± 0.037	6	0.468 ± 0.064	50	0.504 ± 0.262	88
$C_i > 350$	0.038 ± 0.005	0	0.045 ± 0.007	0	0.262 ± 0.024	65	0.132 ± 0.130	70
<i>C. arabica</i>								
$C_i < 100$	0.131 ± 0.018	0	0.202 ± 0.042	10	0.164 ± 0.028	0	0.202 ± 0.035	20
$C_i 100-350$	0.117 ± 0.006	0	0.124 ± 0.007	0	0.186 ± 0.029	0	0.191 ± 0.029	6
$C_i > 350$	0.052 ± 0.004	0	0.053 ± 0.004	0	0.219 ± 0.038	41	0.194 ± 0.039	56
<i>L. gibertii</i>								
$C_i < 100$	0.235 ± 0.027	0	0.270 ± 0.050	7	0.310 ± 0.041	7	0.275 ± 0.079	27
$C_i 100-350$	0.214 ± 0.014	0	0.228 ± 0.020	0	0.371 ± 0.044	7	0.406 ± 0.083	21
$C_i > 350$	0.071 ± 0.011	0	0.073 ± 0.012	0	0.226 ± 0.063	32	0.162 ± 0.044	42

Values are the means ± standard error of 4–6 A/C_i curves per species. The SE was calculated according to the points that remained in each C_i interval after applying the restriction.

counterpart (Table 5). These higher V_{cmax} and J_{max} values are in agreement with the lower g_m values found, in general, with the A/C_i J calibration (Table 4). The V_{cmax} obtained using the Ethier and Livingston method was closer to the V_{cmax} on a C_c basis calculated using the A/C_i J calibration for *L. gibertii* and *C. arabica*, whereas for *N. tabacum* an intermediate value between those obtained with the A/PPFD or A/C_i J calibration was found (Table 5). Apart from the J_{max} calculated with the A/C_i J calibration, which had the higher values for all species and reflected the higher $\alpha\beta$ found (Table 3), there were no major differences among the other calculated values of J_{max} . The use of the standard Rubisco kinetics (K_c , K_o , and Γ^*) originally obtained for *N. tabacum* by Bernacchi *et al.* (2002) would lead to an overestimation of V_{cmax} by ~30% and 20% for *L. gibertii* and *C. arabica*, respectively. The other photosynthetic parameters for these two species were unaffected by the use of different Rubisco kinetic constants (Table 5). No significant differences were observed for *N. tabacum* when using the different set of Rubisco kinetics, with the exception of g_m (Ethier and Livingston method), which was 28% lower when using the Rubisco kinetics of Bernacchi *et al.* (2002).

Discussion

To the best of the authors' knowledge, this study is the first to address the idea that the use of A/C_i or A/PPFD curves under low O₂ to calibrate J can significantly affect the estimations of g_m , V_{cmax} , and J_{max} , as demonstrated in species with contrasting leaf structural properties and photosynthetic capacities. A background is also provided to understand potential factors that could be translated into unrealistic g_m values at low and high C_i , and recommendations to improve g_m estimations accordingly.

Sensitivity of the variable J method to $\alpha\beta$

The high sensitivity of the variable J method has been known since its introduction by Harley *et al.* (1992). However, among the several sources of error, more attention has been given to an accurate determination of Γ^* (Warren *et al.*, 2006; Pons *et al.*, 2009) than to J *per se*, given the variety of ways in which J can be calibrated. Despite the J calibration based on A/PPFD curves being the most common method in the literature, here it is shown that this calibration produced a higher number of unrealistic g_m estimates than its counterpart based on A/C_i curves (Table 4). Additionally, it was demonstrated that g_m misestimations could be directly associated with the J calibration method at high C_i on the one hand, and the proper choice of Γ^* and R_L at low C_i on the other hand. Notably, the need to develop useful criteria to improve g_m estimations and to understand the high g_m variability is crucial considering that the only existing indicator, the Harley *et al.* (1992) criteria which consider that reliable g_m estimations are those situated in the range of dC_c/dA (10–50), performed poorly in retrieving acceptable data in addition to being dependent on the species, applied C_i range, and J calibration (Supplementary Table S4 at JXB online).

It can be deduced from the relationship between C_c and $J/(A+R_L)$ (Fig. 3A) that C_c approaches infinity as $J/(A+R_L)$ approaches four (number of electrons per CO₂ molecule fixed). In contrast, C_c is negative when the ratio is less than four [the lower C_c threshold for positive $J/(A+R_L)$ is defined by the parameter Γ^*]. Therefore, as $J/(A+R_L)$ approaches four as photorespiration and other alternative electron sinks tend to decrease (at high C_i , for example), extremely high C_c values are to be expected, leading to a greater probability of

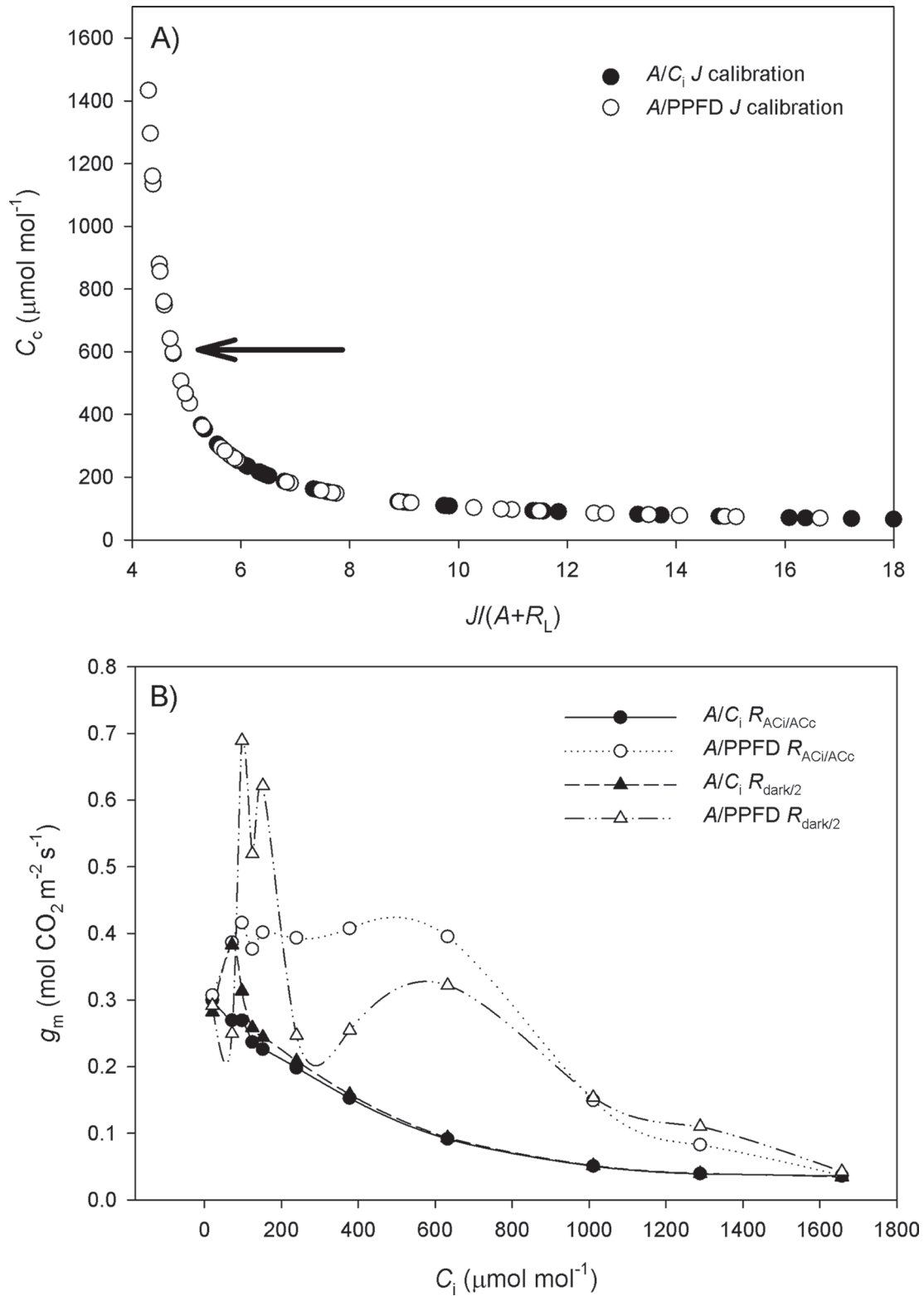


Fig. 3. (A) Relationship between C_c and $J/(A+R_l)$, as affected by the J calibration using the $A/PPFD$ (open circles) or A/C_i curves (filled circles). As $J/(A+R_l)$ approaches four (likely to occur at high C_i), C_c tends to infinity, thus increasing the probability of being higher than C_i and resulting in negative g_m values. The arrow indicates the C_c upper limit ($\sim 600 \mu\text{mol mol}^{-1}$) observed for the A/C_i J calibration, being much lower than its $A/PPFD$ counterpart which can reach C_c values $>1600 \mu\text{mol mol}^{-1}$. (B) g_m response to C_i as affected by the A/C_i (filled symbols) or $A/PPFD$ (open symbols) J calibration method and the light respiration estimations [$R_{\text{dark}/2}$ (triangles) or $R_{ACi/ACc}$ (circles)]. It is remarkable how there are 'spikes' in g_m at low C_i when using $R_{\text{dark}/2}$ and how these are alleviated when using $R_{ACi/ACc}$. The curves are from *L. gibertii*, and the points are averages from four plants for g_m between 0 and $1 \text{ mol CO}_2 \text{ m}^{-2} \text{ s}^{-1}$. The A/C_i or $A/PPFD$ J calibration refers to the $\alpha\beta$ obtained from the curves shown in Fig. 2A and B, respectively.

Table 5. Maximum carboxylation rate of Rubisco (V_{cmax} , $\mu\text{mol CO}_2 \text{ m}^{-2} \text{ s}^{-1}$), maximum electron transport rate from gas exchange (J_{max} , $\mu\text{mol e}^- \text{ m}^{-2} \text{ s}^{-1}$), mesophyll conductance (g_m , Ethier, $\text{mol CO}_2 \text{ m}^{-2} \text{ s}^{-1}$) according to Ethier and Livingston (2004), and electron transport rate estimated from chlorophyll fluorescence (J_{flu} , $\mu\text{mol e}^- \text{ m}^{-2} \text{ s}^{-1}$)

All of the photosynthetic parameters were calculated on a C_i basis from the A/C_i curves or on a C_c basis from the A/C_c curves using the measured Rubisco kinetic constants (Γ^* , K_c , and K_o) in this study (as reported in Table 1) or the standard Rubisco kinetics for tobacco from Bernacchi et al. (2002). A/C_i J cal and $A/PPFD$ J calibration denote the photosynthetic parameters calculated for A/C_c curves using the $\alpha\beta$ retrieved from Φ_{PSII}/Φ_{CO_2} (A/C_i) or ($A/PPFD$) J calibrations. Note that J_{flu} is independent of Rubisco kinetics.

	Measured kinetic constants			Bernacchi constants		
	<i>N. tabacum</i>	<i>C. arabica</i>	<i>L. gibertii</i>	<i>N. tabacum</i>	<i>C. arabica</i>	<i>L. gibertii</i>
V_{cmax} C_i basis	71.7 ± 4.6	41.7 ± 2.4*	70.5 ± 1.6*	59.8 ± 3.8	49.8 ± 2.7	104.0 ± 2.4
V_{cmax} C_c basis A/C_i J cal	106.3 ± 8.9	73.9 ± 3.6*	133.4 ± 11.9*	87.0 ± 7.1	89.8 ± 4.4	210.1 ± 20.8
V_{cmax} C_c basis $A/PPFD$ J cal	80.2 ± 5.7	59.8 ± 3.8*	101.7 ± 8.2*	66.7 ± 4.6	70.3 ± 3.1	155.8 ± 14.0
V_{cmax} Ethier	91.8 ± 14.7	80.2 ± 4.0*	124.8 ± 5.0*	81.7 ± 9.2	102.1 ± 5.4	164.6 ± 11.7
J_{max} C_i basis	87.2 ± 7.4	110.7 ± 3.4	175.3 ± 7.3	86.6 ± 7.4	110.7 ± 3.4	176.6 ± 7.4
J_{max} C_c basis A/C_i cal	103.2 ± 10.5	136.6 ± 7.1	228.6 ± 8.7	101.4 ± 10.3	136.6 ± 7.1	233.4 ± 8.9
J_{max} C_c basis $A/PPFD$ cal	84.9 ± 7.3	113.7 ± 5.7	177.0 ± 5.8	84.4 ± 7.3	113.1 ± 5.3	178.2 ± 5.8
J_{max} Ethier	99.5 ± 3.3	115.0 ± 3.2	179.8 ± 8.9	99.5 ± 3.3	114.4 ± 3.2	179.8 ± 8.9
J_{flu} A/C_i J cal	117.5 ± 11.4	139.2 ± 6.7	236.0 ± 9.7	–	–	–
J_{flu} $A/PPFD$ J cal	94.7 ± 7.9	113.1 ± 4.8	181.7 ± 6.4	–	–	–
g_m Ethier	0.412 ± 0.045	0.108 ± 0.006	0.226 ± 0.036	0.296 ± 0.015	0.101 ± 0.005	0.257 ± 0.048

Values are the means ± standard error of 4–6 A/C_i or A/C_c curves per species.

R_{AC_i/AC_c} was used when needed.

An asterisk denotes differences in the respective photosynthetic parameter calculated using the different set of Rubisco kinetics.

The graphical representation of the A/C_i and A/C_c curves is shown in [Supplementray Figure S1](#) at [JXB](#) online.

estimating negative values of g_m . Thus, for the same ($A+R_L$), the higher the $\alpha\beta$, the higher the J , ultimately resulting in a greater probability of obtaining positive g_m values due to a lowering of C_c , whereas the opposite holds true for a lower $\alpha\beta$.

At low C_i (<100 $\mu\text{mol mol}^{-1}$ air), misestimations of g_m are unlikely to be affected by $J/(A+R_L)$, as this ratio tends to achieve higher values with decreasing C_i . In any case, reliable estimations of g_m at low C_i are extremely challenging given that the estimations are highly dependent on the proper choice of values of Γ^* or R_L , which can ultimately affect C_c . In the present study, the authors are quite confident about their Γ^* values because they were estimated from Rubisco kinetics in purified preparations. Given this, it was possible to retrieve a respiration estimate (R_{AC_i/AC_c}) as the value forcing the intercept of the linear relationship of A versus C_i-C_c to zero, which is equivalent to forcing the Γ to be the same. It is believed that R_{AC_i/AC_c} obtained in this way is a valid estimate, as its magnitude was lower than that of R_{dark} (Table 3), in agreement with the general consensus that respiration is inhibited in the light (Tcherkez et al., 2005). In addition, the use of R_{AC_i/AC_c} significantly improved the number of valid g_m estimates (Table 4), highlighting the importance of respiration in estimating g_m at low C_i , with the advantage of better matching a biochemical prediction of the FvCB model, namely A/C_i and A/C_c sharing the same Γ .

An *a priori* weakness regarding R_{AC_i/AC_c} resides in whether g_m is kept constant at a low C_i range. However, the authors argue in favour of a constant g_m where a high linearity can be observed when plotting A versus C_i-C_c , in the region strictly limited by Rubisco (Fig. 1C). Furthermore, it can also be

noted that g_m estimated using the variable J method is closer to the constant g_m , as the individual points are close to the regression line in the plot of A versus C_i-C_c . The apparent variability of g_m that might be identified using the variable J method could simply be a result of the high sensitivity of A , C_i , or C_c to random errors at this low C_i range. This conclusion is supported when comparing the data of Flexas et al. (2007), who showed a high variability of g_m at low C_i using the variable J method, with those recorded by Tazoe et al. (2011), who found almost constant values of g_m using the isotopic method.

Why do A/C_i and $A/PPFD$ curves result in different $\alpha\beta$?

Given that α can be measured and that large changes in this parameter during the execution of $A/PPFD$ or A/C_i curves are unlikely to occur, the uncertainty in J is particularly related to β . Eichelmann and Laisk (2000) found β varying from 0.38 to 0.51 in *N. tabacum* under varying light and temperature conditions. Similar results were reported by Loreto et al. (2009) while studying the effect of blue light on g_m . Hassiotou et al. (2009) also concluded that J calibration is light dependent. Collectively, all of this information highlights the importance of irradiance in determining the β value and helps explain the apparently better suitability of the A/C_i -based J calibration: it is performed under the same irradiance used in the normal A/C_i curves. In fact, another advantage of keeping a fixed irradiance during the calibration is to avoid changes in the profiles of light absorption through the leaf that may occur under changing irradiance (Evans, 2009; Oguchi et al., 2011); this can be especially important for

the Li-Cor LED-based fluorescence/light source which consists of blue and red light with narrow bandwidths. However, to what extent changes in spectral light could be responsible for differences in β is unclear (Evans, 2009). Further explanations for this statement might be linked to the engagement of alternative electron sinks and the fluorescence signals that might not be representative of the whole leaf, in contrast to the gas-exchange signals (Hassiotou *et al.*, 2009). Even if the uncertainty about the fluorescence signal could be resolved using calibration curves, as in this study, conflicting information on the possible effects of alternative electron sinks on g_m measurements has been reported. Whereas several authors (e.g. Loreto *et al.*, 1994; Ruuska *et al.*, 2000; Flexas and Medrano, 2002) showed circumstantial evidence suggesting that alternative electron sinks play no major role in g_m estimations, other investigators reported that up to 24% of the total electron flux can be associated with alternative sinks (see Gilbert *et al.*, 2012, and references therein). In any case, the present results argue against the relevance of alternative electron sinks as potential bias for proper g_m estimations, given that the calibration methods most likely to be affected by these sinks (calibrations performed at high PPFD and low C_i) did not differ from others which used a range of data under strictly limited electron transport (low PPFD and high C_i).

Mesophyll conductance, maximum velocity of Rubisco carboxylation, and electron transport rate

The choice of the method to calibrate J can significantly affect the estimation of photosynthetic parameters and even alter their interpretation in the context of the diffusive versus biochemical limitations to photosynthesis. In *N. tabacum*, the use of $A/PPFD$ calibration would lead to the conclusion that the assumption of infinite g_m is plausible because no difference in V_{cmax} on a C_i or C_c basis was observed (Table 5). In sharp contrast, the use of A/C_i calibration points to a finite g_m and a higher V_{cmax} value (33%) in relation to the V_{cmax} on a C_i basis. For *C. arabica* and *L. gibertii*, higher V_{cmax} values were observed using both A/C_i and $A/PPFD$ J calibrations compared with V_{cmax} on a C_i basis, but the degree of underestimation varied considerably (Table 5). It is important to bear in mind that such alterations also imply changes in biochemical aspects of the leaf because V_{cmax} is related to the amount of activated Rubisco, whereas J_{max} is associated with components of the electron transport chain, and both parameters can affect the leaf nitrogen economy (Niinemets and Tenhunen, 1997). Thus, it is highly unlikely that both calibrations can hold true, as they can considerably change the leaf biochemical signature and hence ultimately pose uncertainties on how to decide which calibration to use. To address this issue, a first cut-off point is to check if the minimum requirement of four electrons per carboxylation is attained, which can be achieved by dividing J by A . If this ratio is less than four, the calibration is, on a theoretical basis, inadequate. This criterion allowed the exclusion of the standard $\alpha\beta$ for *C. arabica* (Supplementary Table S2 at *JXB* online) and the $A/PPFD$ calibration for *N. tabacum*. In addition, g_m and the FvCB photosynthetic parameters were estimated using the

J -independent Ethier and Livingston method. Interestingly, the values of V_{cmax} and g_m obtained with this method reasonably matched those obtained with the A/C_i J calibration for *L. gibertii* and *C. arabica*. In *N. tabacum*, the V_{cmax} calculated from the Ethier approach presented intermediate values between the V_{cmax} from the $A/PPFD$ or A/C_i calibration, and, given the high standard errors in its g_m estimate, it is believed that, even in this species, the A/C_i J calibration might be a better option to recommend, as it allows the retrieval of a greater number of realistic g_m estimations regardless of the respiration value (Tables 4, 5). Therefore, it is proposed that the A/C_i J calibration seems to be more reliable than its $A/PPFD$ counterpart in terms of producing acceptable data, in accordance with the results of Gilbert *et al.* (2012).

Regarding the use of Rubisco kinetic constants, a considerable overestimation of V_{cmax} (~30%) would occur in *L. gibertii* if standard values of those constants (Bernacchi *et al.*, 2002) were used (Table 5). Importantly, even if good fits could be obtained irrespective of the kinetic constants, the relationship between V_{cmax} and leaf nitrogen might be compromised. Thus, if the main goal is to use the FvCB model to characterize photosynthetic capacities and relate them to nitrogen partitioning (e.g. Xu *et al.*, 2012), species-specific kinetic constants for Rubisco should be implicitly used.

Further recommendations to improve g_m estimation

Given the uncertainties in g_m estimations, criteria were provided to assess the consistency of Γ^* and R_L through the determination of Γ (by definition, Γ must be higher than Γ^*) or by plotting A versus C_i-C_c and analysing the intercept of the linear relationship. In addition, provided that the estimates of Γ and Γ^* are reliable, it is possible to retrieve a respiration estimate from A/C_i and A/C_c curves. The respiration value was the focus here because of the availability of the current methods to estimate R_L using gas exchange and/or chlorophyll fluorescence (see Yin *et al.*, 2011), all of which were performed under low irradiance conditions that do not match those used in A/C_i curves, which ultimately makes the choice of a proper respiration value a very complicated task.

If an inconsistency between Γ for the A/C_i curve and Γ^* (Γ lower than Γ^*) is found, or if the value of respiration retrieved by forcing the intercept of A versus C_i-C_c to zero is negative, four potential sources of error need to be checked: (i) correction for CO_2 and water vapour leakage through the chamber gaskets is crucial to the determination of Γ and very important for species with low photosynthetic potential (see Rodeghiero *et al.*, 2007); (ii) the influence of lateral diffusion can become significant (especially for homobaric leaves) with large gradients of CO_2 inside and outside the chamber in addition to the lower fluxes of CO_2 near the compensation point (Morison and Lawson, 2007); (iii) Γ^* determination; and (iv) Rubisco deactivation. The first two sources of error are particularly dependent on the leaf chamber size and, given the magnitude of the corrections in A at low C_i (Supplementary Table S1 at *JXB* online), the need to use larger leaf chambers to obtain more reliable g_m , Γ , and R_{AC_i/AC_c} estimates is emphasized. For species displaying low

respiration rates, it is possible to obtain an estimate of Γ^* by fixing R_L , inputting a test Γ^* , and changing this parameter to obtain the intercept of A versus $C_i - C_c$ closest to zero. All of these hints provide a good framework to extract as much information as possible from the A/C_i and A/C_c curves. Nevertheless, because all of these adjustments rely on fitting processes, proper judgement about the biological meaning of the obtained estimates is obviously required.

Regarding the J calibration, independent of it being based on A/C_i , $A/PPFD$, or both, one should first check whether all of the positive J/A values are higher than four. If not, there is an inconsistency with the calibration because this implies that fewer than four electrons would be used per carboxylation event. If yes, the next step is to verify the suitability of the respiration value by checking if all of the positive $J/(A+R_L)$ values are still higher than four. If not, there is an inconsistency for the same reason stated previously. Another checkpoint is to verify that the maximum observed C_c is at least equal to the maximum C_i that would implicate infinite g_m . If C_c values higher than the maximum C_i are present for positive A , there is again an inconsistency with the calibration, as Fick's first law of diffusion predicts a drawdown of CO_2 between C_i and C_c . In fact, it is theoretically possible to define an upper limit for $\alpha\beta$ which would be the value making the A/C_i and A/C_c curves identical, implicating infinite g_m .

Conclusion

This work brings new information to the growing amount of published papers trying to improve g_m estimation. Criteria are provided to examine the amount of unrealistic g_m data and identify inconsistencies with the biochemical model utilized, leading to a higher amount of acceptable data. In addition, the need for additional measurements to validate the J calibration to improve the estimation of photosynthetic parameters is emphasized. Moreover, given the observed high variability in g_m , it is important that comparisons among studies reporting data consider the variability due to the J calibration method, and, if necessary, normalize data according to the reported $\alpha\beta$ values.

Supplementary data

Supplementary data are available at *JXB* online.

Figure S1. Graphical representation of the A/C_i and their respective A/C_c curves calibrated with the A/C_i or $A/PPFD$ J calibration.

Table S1. Leakage correction for CO_2 and water vapour.

Table S2. Averaged mesophyll conductance (g_m) for the interval of C_i ranging from 100 to 350 $\mu\text{mol mol}^{-1}$ air and the single point g_m at ambient CO_2 concentration (400 $\mu\text{mol mol}^{-1}$ air) using $R_{\text{dark}/2}$ in the g_m estimation.

Table S3. The same as in **Table S1**, using $R_{A/C_i/A/C_c}$ rather than $R_{\text{dark}/2}$ to estimate g_m .

Table S4. Mesophyll conductance (g_m , $\text{mol CO}_2 \text{ m}^{-2} \text{ s}^{-1}$) for several intervals of C_i and percentage of data excluded (DE) after applying two restrictions (g_m restricted to the range of

$0 < g_m < 1 \text{ mol CO}_2 \text{ m}^{-2} \text{ s}^{-1}$ and dC/dA of 10–50 [the **Harley *et al.* (1992)** criteria].

Table S5. Maximum carboxylation rate of Rubisco (V_{cmax}) and maximum electron transport rate from gas exchange (J_{max}), as affected by the different J calibrations and calculated with $R_{\text{dark}/2}$.

Spreadsheet S1. An Excel spreadsheet is provided that allows the user to retrieve the leaf respiration from combined A/C_i and A/C_c curves.

Acknowledgements

This research was supported by the National Council for Scientific and Technological Development (CNPq) (grant 302605/2010-0) to FMD and Plan Nacional (Spain) (grant AGL2009-07999) to JG. A PhD scholarship granted by CNPq to SCVM is also gratefully acknowledged.

References

- Bernacchi CJ, Portis AR, Nakano H, Von Caemmerer S, Long SP.** 2002. Temperature response of mesophyll conductance. Implications for the determination of Rubisco enzyme kinetics and for limitations to photosynthesis *in vivo*. *Plant Physiology* **130**, 1992–1998.
- Bird IF, Cornelius MJ, Keys AJ.** 1982. Affinity of RuBP carboxylases for carbon dioxide and inhibition of the enzymes by oxygen. *Journal of Experimental Botany* **33**, 1004–1013.
- Brooks A, Farquhar GD.** 1985. Effect of temperature on the CO_2/O_2 specificity of ribulose-1,5-bisphosphate carboxylase/oxygenase and the rate of respiration in the light. *Planta* **165**, 397–406.
- Butz ND, Sharkey TD.** 1989. Activity ratios of ribulose-1,5-bisphosphate carboxylase accurately reflect carbamylation ratios. *Plant Physiology* **89**, 735–739.
- Eichelmann H, Laisk A.** 2000. Cooperation of photosystems II and I in leaves as analyzed by simultaneous measurements of chlorophyll fluorescence and transmittance at 800 nm. *Plant and Cell Physiology* **41**, 138–147.
- Edwards GE, Baker NR.** 1993. Can CO_2 assimilation in maize leaves be predicted accurately from chlorophyll fluorescence analysis? *Photosynthesis Research* **37**, 89–102.
- Ethier GJ, Livingston NJ.** 2004. On the need to incorporate sensitivity to CO_2 transfer conductance into the Farquhar–von Caemmerer–Berry leaf photosynthesis model. *Plant, Cell and Environment* **27**, 137–153.
- Evans JR.** 2009. Potential errors in electron transport rates calculated from chlorophyll fluorescence as revealed by a multilayer leaf model. *Plant and Cell Physiology* **50**, 698–706.
- Evans JR, von Caemmerer S.** 1996. Carbon dioxide diffusion inside leaves. *Plant Physiology* **110**, 339–346.
- Farquhar GD, von Caemmerer S, Berry JA.** 1980. A biochemical model of photosynthetic CO_2 assimilation in leaves of C3 species. *Planta* **149**, 78–90.
- Flexas J, Barbour MM, Brendel O, et al.** 2012. Mesophyll diffusion conductance to CO_2 : an appreciated central player in photosynthesis. *Plant Science* 193–194, 70–84.

- Flexas J, Diaz-Espejo A, Galmés J, Kaldenhoff R, Medrano H, Ribas-Carbo M.** 2007. Rapid variations of mesophyll conductance in response to changes in CO₂ concentration around leaves. *Plant, Cell and Environment* **30**, 1284–1298.
- Flexas J, Medrano H.** 2002. Energy dissipation in C₃ plants under drought. *Functional Plant Biology* **29**, 1209–1215.
- Flexas J, Ribas-Carbó M, Diaz-Espejo A, Galmés J, Medrano H.** 2008. Mesophyll conductance to CO₂: current knowledge and future prospects. *Plant, Cell and Environment* **31**, 602–621.
- Harley PC, Loreto F, Di Marco G, Sharkey TD.** 1992. Theoretical considerations when estimating the mesophyll conductance to CO₂ flux by analysis of the response of photosynthesis to CO₂. *Plant Physiology* **98**, 1429–1436.
- Hassiotou F, Ludwig M, Renton M, Veneklaas EJ, Evans JR.** 2009. Influence of leaf dry mass per area, CO₂, and irradiance on mesophyll conductance in sclerophylls. *Journal of Experimental Botany* **60**, 2303–2314.
- Galmés J, Flexas J, Keys AJ, Cifre J, Mitchell RAC, Madgwick PJ, Haslam RP, Medrano H, Parry MAJ.** 2005. Rubisco specificity factor tends to be larger in plant species from drier habitats and in species with persistent leaves. *Plant, Cell and Environment* **28**, 571–579.
- Galmés J, Medrano H, Flexas J.** 2006. Acclimation of Rubisco specificity factor to drought in tobacco: discrepancies between *in vitro* and *in vivo* estimations. *Journal of Experimental Botany* **57**, 3659–3667.
- Galmés J, Medrano H, Flexas J.** 2007. Photosynthetic limitations in response to water stress and recovery in Mediterranean plants with different growth forms. *New Phytologist* **175**, 81–93.
- Genty B, Briantais JM, Baker NR.** 1989. The relationship between the quantum yield of photosynthetic electron-transport and quenching of chlorophyll fluorescence. *Biochimica et Biophysica Acta* **990**, 87–92.
- Gilbert ME, Pou A, Zwieniecki MA, Holbrook NM.** 2012. On measuring the response of mesophyll conductance to carbon dioxide with the variable *J* method. *Journal of Experimental Botany* **63**, 413–425.
- Laisk A, Loreto F.** 1996. Determining photosynthetic parameters from leaf CO₂ exchange and chlorophyll fluorescence. *Plant Physiology* **110**, 903–912.
- Loreto F, Marco G, Tricoli D, Sharkey T.** 1994. Measurements of mesophyll conductance, photosynthetic electron transport and alternative electron sinks of field grown wheat leaves. *Photosynthesis Research* **41**, 397–403.
- Loreto F, Tsonev T, Centritto M.** 2009. The impact of blue light on leaf mesophyll conductance. *Journal of Experimental Botany* **60**, 2283–2290.
- Morison JIL, Lawson T.** 2007. Does lateral gas diffusion in leaves matter? *Plant, Cell and Environment* **30**, 1072–1085.
- Niinemets U, Cescatti A, Rodeghiero M, Tosens T.** 2005. Leaf internal diffusion conductance limits photosynthesis more strongly in older leaves of Mediterranean evergreen broad-leaved species. *Plant, Cell and Environment* **28**, 1552–1566.
- Niinemets U, Cescatti A, Rodeghiero M, Tosens T.** 2006. Complex adjustments of photosynthetic potentials and internal diffusion conductance to current and previous light availabilities and leaf age in Mediterranean evergreen species *Quercus ilex*. *Plant, Cell and Environment* **29**, 1159–1178.
- Niinemets U, Díaz-Espejo A, Flexas J, Galmés J, Warren CR.** 2009a. Role of mesophyll diffusion conductance in constraining potential photosynthetic productivity in the field. *Journal of Experimental Botany* **60**, 2249–2270.
- Niinemets U, Flexas J, Peñuelas J.** 2011. Evergreens favored by higher responsiveness to increased CO₂. *Trends in Ecology and Evolution* **26**, 136–142.
- Niinemets U, Tenhunen JD.** 1997. A model separating leaf structural and physiological effects on carbon gain along light gradients for the shade-tolerant species *Acer saccharum*. *Plant, Cell and Environment* **20**, 845–866.
- Niinemets U, Wright IJ, Evans JR.** 2009b. Leaf mesophyll diffusion conductance in 35 Australian sclerophylls covering a broad range of foliage structural and physiological variation. *Journal of Experimental Botany* **60**, 2433–2449.
- Oguchi R, Douwstra P, Fujita T, Chow WS, Terashima I.** 2011. Intra-leaf gradients of photoinhibition induced by different color lights: implications for the dual mechanisms of photoinhibition and for the application of conventional chlorophyll fluorometers. *New Phytologist* **191**, 146–159.
- Pons TL, Flexas J, Von Caemmerer S, Evans JR, Genty B, Ribas-Carbó M, Brugnoli E.** 2009. Estimating mesophyll conductance to CO₂: methodology, potential errors, and recommendations. *Journal of Experimental Botany* **60**, 2217–2234.
- Rodeghiero M, Niinemets U, Cescatti A.** 2007. Major diffusion leaks of clamp-on leaf cuvettes still unaccounted: how erroneous are the estimates of Farquhar *et al.* model parameters? *Plant, Cell and Environment* **30**, 1006–1022.
- Ruuska SA, Badger MR, Andrews TJ, von Caemmerer S.** 2000. Photosynthetic electron sinks in transgenic tobacco with reduced amounts of Rubisco: little evidence for significant Mehler reaction. *Journal of Experimental Botany* **51**, 357–368.
- Seaton GGR, Walker DA.** 1990. Chlorophyll fluorescence as a measure of photosynthetic carbon assimilation. *Proceedings of the Royal Society B: Biological Sciences* **242**, 29–35.
- Sharwood RE, von Caemmerer S, Maliga P, Whitney SM.** 2008. The catalytic properties of hybrid Rubisco comprising tobacco small and sunflower large subunits mirror the kinetically equivalent source Rubiscos and can support tobacco growth. *Plant Physiology* **146**, 83–96.
- Tazoe Y, von Caemmerer S, Estavillo GM, Evans JR.** 2011. Using tunable diode laser spectroscopy to measure carbon isotope discrimination and mesophyll conductance to CO₂ diffusion dynamically at different CO₂ concentrations. *Plant, Cell and Environment* **34**, 580–591.
- Tcherkez G, Cornic G, Bligny R, Gout E, Ghashghaie J.** 2005. *In vivo* respiratory metabolism of illuminated leaves. *Plant Physiology* **138**, 1596–1606.
- Tosens T, Niinemets Ü, Westoby M, Wright IJ.** 2012. Anatomical basis of variation in mesophyll resistance in eastern Australian sclerophylls: news of a long and winding path. *Journal of Experimental Botany* **63**, 5105–5119.

Valentini R, Epron D, Angelis P, Matteucci G, Dreyer E. 1995. *In situ* estimation of net CO₂ assimilation, photosynthetic electron flow and photorespiration in Turkey oak (*Q. cerris* L.) leaves: diurnal cycles under different levels of water supply. *Plant, Cell and Environment* **18**, 631–640.

Warren CR, Adams MA. 2004. Evergreen trees do not maximize instantaneous photosynthesis. *Trends in Plant Science* **9**, 270–274.

Warren CR. 2006. Estimating the internal conductance to CO₂ movement. *Functional Plant Biology* **33**, 431–442.

Xu C, Fisher R, Wullschlegel SD, Wilson CJ, Cai M, McDowell NG. 2012. Toward a mechanistic modeling of nitrogen limitation on vegetation dynamics. *PLoS One* **7**, e37914

Yin X, Struik PC, Romero P, Harbinson J, Evers JB, van der Putten PEL, Vos J. 2009. Using combined measurements of gas exchange and chlorophyll fluorescence to estimate parameters of a biochemical C₃ photosynthesis model: a critical appraisal and a new integrated approach applied to leaves in a wheat (*Triticum aestivum*) canopy. *Plant, Cell and Environment* **32**, 448–464.

Yin X, Sun Z, Struik PC, Gu J. 2011. Evaluating a new method to estimate the rate of leaf respiration in the light by analysis of combined gas exchange and chlorophyll fluorescence measurements. *Journal of Experimental Botany* **62**, 3489–3499.

Yin X, van Oijen M, Schapendonk AHCM. 2004. Extension of a biochemical model for the generalized stoichiometry of electron transport limited C₃ photosynthesis. *Plant, Cell and Environment* **27**, 1211–1222.